Journal of Cellular Biochemistry 99:305–318 (2006)

Molecular Dynamics Simulation and Automated Docking of the Pro-Apoptotic Bax Protein and its Complex With a Peptide Designed From the Bax-Binding Domain of Anti-Apoptotic Ku70

Fabrizio Mancinelli,[1] Michele Caraglia,[2]* Alfredo Budillon,[2] Alberto Abbruzzese,[1] and Ettore Bismuto[1]**

[1]Department of Biochemistry and Biophysics, Seconda Università degli Studi di Napoli, 80138 Napoli, Italy
[2]Department of Experimental Pharmacology, National Institute of Tumours ''Fondazione G. Pascale,'' Naples, Italy

Abstract Bax, a multi-domain protein belonging to the large family of Bcl-2 proteins, has a pivotal role for the initiation of the cytochrome *c*-mediated apoptosis, a vital physiologic process to eliminate damaged or unwanted cells. In response to specific stimuli Bax translocates from cytosol to mitochondria outer membrane where a process of oligomerization occurs with pore formation through which cytochrome *c* and other death molecules escape. The pro-death action of Bax is regulated by the interaction with other pro-survival proteins. However, the conformational changes and the structural details necessary for homo and hetero interaction with other regulating proteins are largely unknown. This article reports a combined investigation of molecular dynamics (MD) simulation and automated docking that evidence the molecular regions of Bax involved in the binding with anti-apoptotic exapeptide (Bip) designed from Ku70, a subunit of the protein complex essential for non-homologous DNA repair but that inhibits also the Bax translocation to mitochondria. Since Bip suppresses apoptosis induced by several anti-cancer drugs, it appears relevant to achieve a better understanding of the structural and dynamical aspects that characterize the Bip–Bax complex in view of potential therapeutic implications. The present results show that the Bax region with the highest affinity for Bip is located in proximity of BH3 homology domain of Bax and also involves the α-helices 1 and 8. Moreover, the comparison of essential motions of Bax at 300 and 400 K before and after the formation of the complex with Bip evidences how the binding with the exa-peptide affects the collective motions of specific molecular districts of Bax considered to have functional relevance. J. Cell. Biochem. 99: 305–318, 2006.

Key words: molecular dynamics; essential dynamics; automated docking; apoptosis; Bax; Bax inhibiting peptide

Programmed cell death, or apoptosis, is a physiological process that plays a critical role in the normal development and maintenance of tissue homeostasis by eliminating infected, mutated, or damaged cells in essentially all multi-cellular organisms. The morphological features that characterize apoptotic cells are shrinkage, plasma membrane bubbling, chromatin condensation, nuclear membrane breakdown, and formation of small vesicles from the cell surface also known as apoptotic bodies [Jiang and Wang, 2004]. The apopoptic machinery in humans consists of a molecular network of a large number of proteins [Cory and Adams, 1998; Danial and Korsmeyer, 2004; Petros et al., 2004]. These proteins regulate a cascade of events in signaling, commitment, and execution stages of apoptosis in through multiple parallel pathways. Defects in key regulators of the

Grant sponsor: Italian Ministry of University and Scientific and Technology Research; Grant number: PRIN2004.

*Correspondence to: Michele Caraglia, Experimental Oncology Department, Experimental Pharmacology Unit, National Cancer Institute Fondazione "G. Pascale," Via M. Semmola, 80131 Naples, Italy.
E-mail: michele.caraglia@fondazionepascale.it

**Correspondence to: Ettore Bismuto, Department of Biochemistry and Biophysics, Seconda Università degli Studi di Napoli, Via de Crecchio 7, 80138 Napoli, Italy.
E-mail: ettore.bismuto@unina2.it

Received 11 November 2005; Accepted 16 February 2006
DOI 10.1002/jcb.20893

complex apopoptic machinery cause anomalous cell growth and cell turnover on which numerous diseases base. These defects can allow neoplastic cells to live beyond their normal lifespan, accumulate genetic mutations, sustain growth under hypoxia and oxidative stress conditions [Schmitt, 2003; Yu and Zhang, 2003]. Conversely, other neurodegenerative disorders such as Alzheimer's, Parkinson's, and Huntington's diseases are characterized by premature loss of specific neurons that causes irreversible memory loss, uncontrolled muscular movements, and depression [Matson, 2000]. Two main parallel and interacting pathways are known by which death signals are trasduced in vertebrates [Nam et al., 2004]: (a) an extrinsic pathway in which the activation of cell surface receptors stimulates the assembly of the death-inducing signaling complex (DISC), within which procaspase-8, a member of cysteine proteases family which orchestrate the dismantling and clearance of the dying cell, is activated [Earnshow et al., 1999]; (b) an intrinsic pathway that involves the translocation following an apopoptic stimulus of pro-apopoptic Bcl-2 proteins, such as Bax, to the mitochondria that triggers the release of cytochrome *c* [Jiang and Wang, 2004]. The release of cytochrome *c* stimulates the Apaf-1 dependent activation of procaspase-9 in the apoptosome that starts the downstream pathway. Cytochrome *c* release from mitochondria is in turn regulated by the interaction of pro- and anti-apoptotic members of the Bcl-2 family of proteins in the cytosol and through the formation of ion-conducting pores at the mitochondrial surface that influence cell fate by regulating mitochondrial physiology. The protein belonging to Bcl-2 family (that can be pro-survival or pro-apopoptic) is based on the presence of one or more "Bcl-2 Homology" (BH) regions. Four of these regions (BH1-4) of sequence homology have been identified, and each Bcl-2 family member contains at least one of them [Petros et al., 2004]. The three-dimensional structure of Bax consists of two central hydrophobic α-helices surrounded by seven amphipathic α-helices of varying lengths. The structures of Bax and other Bcl-2 proteins show a striking similarity to the overall fold of the pore-forming domains of the bacterial toxins and there were reported experimental evidences that they form pores in artificial membranes [Saito et al., 2000]. A prominent hydrophobic groove is present on the surface of the anti-apoptotic proteins. This groove is the binding site for peptides that mimic the BH3 region of various pro-apoptotic proteins such as Bak and Bad [Petros et al., 2004]. Structures of Bcl-x_L in complex with these BH3 peptides show that they bind as an amphipathic α-helix and make extensive hydrophobic contacts with the protein [Zha et al., 1996]. In the pro-apoptotic BH1-3 Bax protein, the hydrophobic groove mainly formed by α-helix segments 4, 5, 6, 7, and 8 is covered by interacting with an additional carboxy-terminal α-helix 9 [Suzuki et al., 2000]. Bax is normally found soluble in the cytoplasm but, at the onset of apoptotic stimuli, migrate to the mitochondria and promote the release of cytochrome *c* and other apoptogenic proteins. The inhibition of Bax apoptoptic-action by binding with Ku70, a subunit of the protein complex essential for non-homologous DNA double-strand break repair [Sawada et al., 2003a], and even by binding small peptides from its Bax-binding domain designed, have been given recently by Sawada et al. [Walker et al., 2001; Sawada et al., 2003b]. They have demonstrated that Ku70 overexpression blocked the mitochondrial translocation of Bax in mammalian cells, but it was enhanced by downregulation of Ku70 [Walker et al., 2001]. More specifically, Sawada et al. [2003b] have found, on the basis of experiments performed on appropriate mutant forms of Bax, that the carboxyl terminus of Ku70 and amino terminus of Bax are required for their interaction. Further evidences [Walker et al., 2001] have shown that only short sequences of Ku70 are necessary to inhibit Bax-mediated apoptosis. These Bax-inhibiting peptides are comprised of five/six amino acids designed from the Bax-binding domain of Ku70 (from residue 578 to residue 583, i.e., VPMKLE). The understanding how Bip acts on Bax molecule could provide valuable information in the development of therapeutics that control apoptosis-related diseases. The results reported in this article were performed by combining molecular dynamics (MD) simulation and automatic docking procedures [Morris et al., 1998; Lindahl et al., 2001], that gave information about the Bax protein regions involved in the formation of the complex of Bax with Bip at 300 K. Moreover, in order to investigate about the nature of the conformational change induced in Bax by apopoptic stimuli a 10 ns trajectory of protein atoms at room temperature and at 400 K was analyzed to

identify among thermal induced conformational motions of Bax those corresponding to functional movements in active form of Bax favoring the homo and dimer formation. With this aim, the trajectories of all atoms of Bax protein were analyzed extracting the essential degrees of freedom according to the method of the Essential Dynamics (ED) Analysis [Amadei et al., 1993]. This method allows a separation of the configurational space into two subspaces: an essential one of very low dimensionality, in which we evidenced collective motions of constituting protein groups with functional implications and the remaining high dimensional one, characterized by nearly constrained gaussian-like thermal fluctuations. The results of docking and ED performed on the complex of Bax with the exa-peptide derived from Ku70 show how the binding with the exa-peptide affects the collective motions of specific molecular districts of Bax having functional relevance [Murphy et al., 2000; Mikhailov, 2003]. Specifically these regions concern: (a) a segment inside N-terminus and α1 helix, supposed to have an important role to start the interaction with the external membrane of mitochondria [Murphy et al., 2000]; (b) the binding region for Bip; (c) the α9 helix whose displacement is necessary for the access to the hydrophobic groove able to interact with the BH3 domain of Bax or other Bcl-2 proteins in the oligomerization process at the mithocondria [Mikhailov, 2003].

METHODS

MD Simulations

All MD simulations were performed with GROMACS (GROningen Machine for Chemical Simulations) v.3.2 and united-atom forcefield [van der Spoel et al., 2004]. The starting configuration of Bax was obtained by averaging the NMR structures [Suzuki et al., 2000] (Protein Data Bank: entry 1F16, X. Liu, S. Dai, Y. Zhu, P. Marrack, J. W. Kappler) with routines included in MOLMOL package [Koradi et al., 1996]. In preparation for the MD simulations Bax protein was placed in the center of a rhombic dodecahedron box of approximate dimensions ($8.05 \times 8.05 \times 5.69$ nm^3) The minimum distance between the protein and the edge of the box was 0.8 nm. All water molecules with their oxygen closer than 0.23 nm to any non-hydrogen protein atom or crystal water oxygen were removed. Three sodium counterions were added to each simulation box to maintain electroneutrality. The box was full of equilibrated SPC rigid water molecules (Single Point Charge, that is, with a partial charge on each of the three constituting atoms). For all MD simulations, initial velocities were taken from a Maxwellian distribution at 300 and 400 K, respectively. Simulations were performed keeping temperature and pressure coupled to external reference, using a Berendsen thermostat and barostat [Berendsen et al., 1984]; coupling constants were 0.1 and 1.0 ps, respectively. All molecular groups (protein, water, and counterions) were coupled independently. Long-range electrostatic interactions were calculated using the Particle Mesh Ewald (PME) method [Luty et al., 1995] with a 9 Å cut-off. The LINear Constraint Solver (LINCS) algorithm [Hess et al., 1997] was used to restrain bond lengths. In order to relief unfavorable non-bonded interactions with the added water molecules each system were energy minimized by a steepest descent algorithm followed by a short 100 ps simulation during which the protein and non-hydrogen atoms were harmonically restrained with a force constant of 1,000 kJ/mol $\cdot$ nm^2. All restraints were then removed and each simulation was run for 10 ns saving co-ordinates and velocities every 5 ps for subsequent analysis. Typical CPU times on dual processor Intel Pentium 4 PCs running Linux Kernel 2.6.3-7 were 2 days per ns. The simulated system comprised 1,902 protein atoms and 11,220 water molecules. The simulation was stopped after 10 ns (including equilibration). As discussed below, the first nanosecond of each simulation is treated as an equilibration period and is not considered in the analysis. To assess the stability of the simulations, the root-mean-square positional deviation (RMSD) of protein atoms with respect to the X-ray structure, the solvent accessible surface area, and the presence of secondary structure elements were monitored.

ED Analysis

The trajectories were further analyzed extracting the essential degrees of freedom according to the method of the Principal Components Analysis, also known as ED [Amadei et al., 1993]. This method is performed by diagonalizing the covariance matrix C of atomic

fluctuations providing a set of eigenvectors and eigenvalues.

It is defined by:

$$C_{ij} = < (q_i - < q_i >)(q_i - < q_j >) >$$

where q_i designates one of the three Cartesian coordinates of one of all atoms in the molecule, and $<q_i>$ is the average value of this coordinate over the ensemble of configurations considered in the analysis. Diagonalization of this matrix affords a set of eigenvector and eigenvalue pairs in which the eigenvector describes the direction of concerted atomic motions in the molecule (a mode), and the eigenvalue characterizes the amplitude of this motion with respect to the eigenvectors. The atomic components of an eigenvector provide a quantitative measure of the participation of each atom to the collective motion described by the corresponding eigenvector. The fluctuations along an eigenvector, η_j; during the MD simulation can be obtained by projecting each frame, I, of the trajectory onto this eigenvector. The value of the projection, p_{ij}, is calculated as:

$$p_{ij} = (x_i - < x >) \cdot \eta_i = \Delta x_i \cdot \eta_i = \sum \Delta x_{ik} \cdot \eta_{jk}$$

where k ranges from 1 to $3 \times$ N; x_i represents a $3 \times$ N dimensional vector containing the atomic coordinates for the ith frame in the trajectory and $<x>$, contains the coordinates of the average structure for the trajectory used to perform the ED analysis.

Docking Simulations

Automated docking simulations were conducted with AutoDock v3.0 [Morris et al., 1998] (Scripps Research Institute, La Jolla, CA) using the NMR structure or crystal structures to generate atomic grids. All water molecules were removed. The programs in AutoDock Tools [Sanner et al., 1999] were used to prepare the ligand for docking. The Hydrogen atoms addition and Gasteiger charges [Gasteiger and Marsili, 1980] were assigned to the ligand using the AutoDock Tools package and the AutoDock software was used to produce final docked conformations within a fixed protein structure. Genetic-Lamarckian algorithms use ideas based on the evolution biology. The particular arrangement of the ligand and the protein can be defined by a set of values describing the translation, orientation, and conformation of the ligand with respect to the protein having a fixed conformation. Each set of ligand value corresponds to a gene, whereas the atomic coordinates correspond to a phenotype. The docking fitness is based on the total interaction energy of the ligand with protein. Selection of offspring is determined by performing on random pair of individual events of crossover, mutation, and by using an adaptive local search method that takes into account the recent history of interaction energy. More specifically, for each docking was selected a population of 100 individuals; the elitism (number of top individuals to survive to the next generation) was 1; the mutation rate was 0.02 and the crossover rate was 0.08.

RESULTS

MD

The MD simulation performed on Bax molecule at 300 K produced a 10 ns trajectory file of all protein atoms. The starting atomic coordinates were obtained by averaging the 20 NMR representative structures (PDB entry: 1F16) [Suzuki et al., 2000] followed by energy minimization using MOLMOL v2K.2 package [Koradi et al., 1996]. Figure 1, top shows the root mean square deviation (RMSD) relative to all atoms of the protein structure at each time (solid line) compared to the initial reference structure. The 300 K trajectory shows an initial jump (within first nanosecond) of about 0.4 nm as consequence of a relaxation of the starting protein structure; afterwards the trajectory is asymptotically stabilized with small fluctuations. The plot of root mean square fluctuation (RMSF, i.e., standard deviation) relatively to each residue in the polypeptide chain of Bax (solid line in Fig. 1, bottom) shows how the atomic fluctuations are distributed for each residue along the protein structure. Seven short segments show higher flexibility, that is, N and C termini, and the segments composed of the residues 35–55, 84–88, 105–109, 155–160, 168–173. The localization of these flexible regions in the three-dimensional structure of Bax after MD simulation can be obtained by the help of Figure 2. This figure shows, in the upper part, the Bax structure with a different color for each α-helix. The protein sequence is reported in the lower part of the same figure in which the α-helix regions are evidenced by lines of the same color shown in the upper part of the figure. As further detail, the homology BH domains are

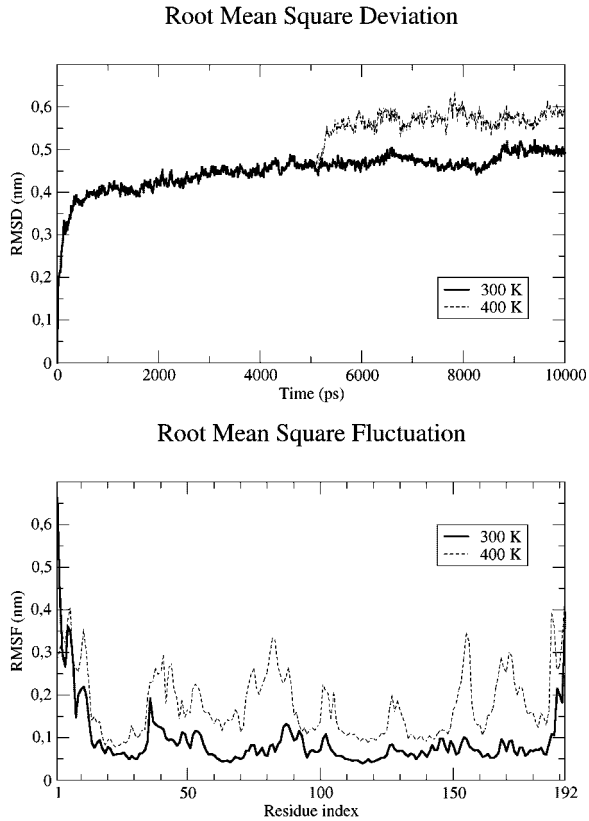

Fig. 1. **Top**: Structural drift of Bax at 300 K (solid line) and 400 K (dashed line) temperatures, shown as root mean square deviation of all atoms. **Bottom**: Fluctuation along the whole trajectory of the C_α of Bax at 300 K (solid line) and 400 K (dashed line) temperatures.

marked by shading in the sequence. Most of the flexible residues of Bax are inside loops between α-helices. With the aim that thermal perturbation could evidence protein motions involving conformational changes that explain the nature of the events activating Bax, a further step of 5 ns dynamic simulation of Bax was performed at 400 K. Figure 1 shows the corresponding RMSD and RMSF of the 400 K trajectory (dashed lines). The analyses were performed on the 400 K MD trajectory with the exclusion of the first nanosecond data. The RMSF dashed lines in Figure 1, bottom shows that although fluctuations are higher compared to those at 300 K (solid line) a large similarity in the shape exists. However, relevant differences can be observed among the regions relative to N and C termini and to the short sequences 60–90, 150–160, and 165–175. Table I summarizes the comparison at 300 and 400 K, respectively, among some structural properties relative to the indicated regions of Bax protein such as helix length, number of hydrogen bonds, and solvent accessible surface per atom. These parameters have been specified for each α-helix segment and for other relevant parts of the protein molecule such as N-terminus and the long loop between α1 and α2 helices. At 300 K, a large part of helical segments (4–9) forms a structural core of Bax protein with poor solvent accessibility. Most of these structural characteristics hold also at 400 K but with different values in the solvent accessibility per atom that in general increases (with the exceptions of α1 and α7 helices) while the number of hydrogen bonds decreases: in particular, for α2, α3, α7, α8 helices hydrogen are drastically reduced with shortening of the corresponding helical segments in some cases. The differences reported in the table about the helices 2, 3 and 7, 8 appear particularly interesting because the first pair of helices (i.e., 2,3) forms the BH3 homology domain, while the differences in the other ones (i.e., 7,8) allow a displacement of helix 9 that rules the access to the hydrophobic groove composed of 4-8 α-helices bundle.

Docking and MD Simulation Between Bax Protein and Bip Peptide

Bax molecule has a central role in the regulation of cytochrome c mediated apoptosis. A mechanism for modulating the Bax activity in the cell is to bind Bax molecules with specific peptides or proteins. This binding can inhibit the interaction of Bax with apoptosis stimulating molecules [Danial and Korsmeyer, 2004]. What regions of Bax structure are involved in the interactions with such regulatory molecules are not well known. To investigate about the molecular regions involved in the binding between Bax and Ku70 or Bip [Walker et al., 2001; Sawada et al., 2003b] we performed automated docking simulations. Docking was carried out by AutoDock suite of programs [Morris et al., 1998] using the Lamarckian genetic algorithm with settings as already specified in the methods section. A preliminary docking search was performed considering the whole macromolecule surface. AutoDock consider the macromolecule as a rigid structure while performing the ligand adaptation. Thus, to take into account for the flexibility of Bax macromolecule we performed AutoDock search on ten different frames of the MD trajectory of Bax from 2 to 10 ns. Each PDB structure

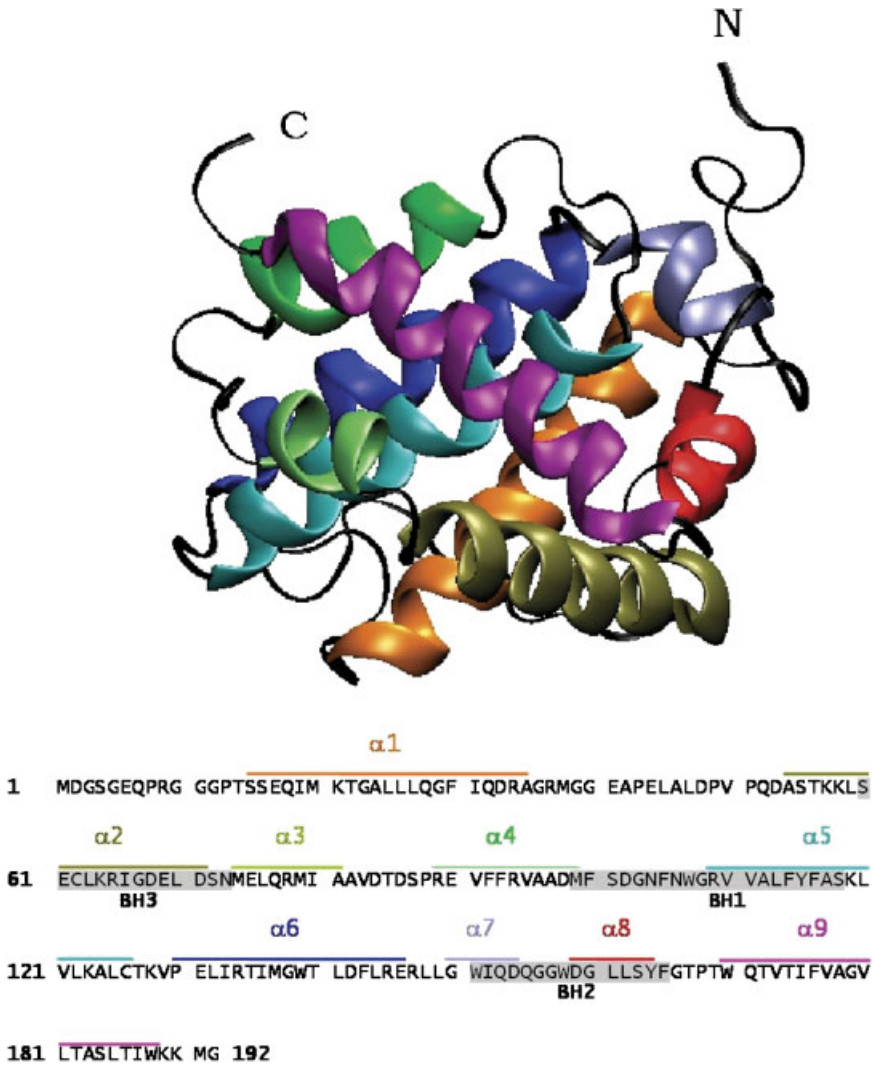

Fig. 2. 3D structure of Bax protein as results from the 10 ns molecular dynamics calculation. In the lower panel the amino-acidic sequence of the protein is explicited; shading identifies the BH binding domains. Secondary structure elements (mainly α-helices) are evidenced by the same colors both in the 3D structure and in the sequence. [Color figure can be viewed in the online issue, which is available at www.interscience.wiley.com.]

TABLE I. Structural Properties of Bax Along the 300 K and 400 K Molecular Dynamics

Secondary structure element	Residues per SS element		H-bonds		SAS/atom ($\times 10^{-2}$ nm^2)	
	300 K	400 K	300 K	400 K	300 K	400 K
N-ter	1–15	1–15	1; 2[a]	1; 1[a]	6.11	6.32
α1	16–34	16–33	2; 15[a]	2; 14[a]	4.25	3.77
Loop α1–α2	35–53	34–53	3; 1[a]	7; 1[a]	6.56	7.01
α2	54–71	54–71	8; 14[a]	10; 11[a]	5.03	5.92
α3	75–82	75–78	4; 4[a]	5	6.49	6.91
α4	88–99	89–99	5; 7[a]	5; 6[a]	3.93	4.68
α5	107–125	107–125	8; 15[a]	7; 15[a]	2.68	3.10
α6	129–147	130–147	4; 16[a]	4; 15[a]	4.29	5.06
α7	151–154	152–153	6	1	4.54	3.03
α8	158–165	158–165	3; 4[a]	1; 4[a]	3.59	4.84
α9	171–185	170–185	4; 11[a]	3; 12	4.20	5.14

[a]Interactions within the considered SS element.

relative to a selected MD frame of the trajectory was included in a grid surrounding both the whole Bax protein and the Bip exa-peptide ligand of $81 \times 81 \times 81$ points spaced 0.0750 nm. The ligand starting conformation of Bip was the same assumed in the crystal structure of Ku70 molecule. In this docking search a limited number of internal rotations and torsions were allowed to Bip (roto-translational degree of freedom). Figure 3 shows the relative histograms representing the binding free energies of clustered docked structure of Bip–Bax complex on the basis of the RMSD (structures in which the total RMSD differ less than 1.0 nm). Each cluster in the figure is located on the basis of the minimum energy among the docked structures forming the cluster. This picture gives a dynamic representation of the ligand-macromolecule adaptation. In fact, observing Figure 3, from bottom to top, it is possible to point out a redistribution of cluster population and shifts in the docking energy scale. Only a single docking site, with the minimum energy (−41.8 kJ/mol), is observed in the histogram representing the Bax conformation after 8 ns dynamic simulation. Therefore, the Bax structure after 8 ns MD was used to start further more refined dockings in which the maximum in the degrees of freedom (25 relative to internal rotations and torsions with the exclusion of the peptide bonds) were allowed and explored Bax surface was appropriately limited. Specifically, the space surrounding the surface of the Bax structure after 8 ns all atoms MD trajectory was divided in four regions (partially overlapping to exclude boundary effects) and explored individually. A grid of $126 \times 126 \times 126$ points, with grid-point spacing of 0.0250 nm, was built in each region. The results of the four refined dockings were summarized in the four histograms shown in Figure 4. The histogram relative to the best cluster of docked structures has reported in the upper left of the figure. The left side of Figure 5 shows the binding site for Bip in the cluster of minimum energy for each explored regions of the space volume surrounding Bax in the same order of the histograms in Figure 4. The best docking for Bip–Bax complex was obtained between Bip and a Bax region located after the N-terminal region (α1) and involving the BH3 and partially BH2 domains (Fig. 5, configuration a); the docking energy was −51.61 kJ/mol. To better refine the structural details of Bip–Bax Bip–Bax complex,

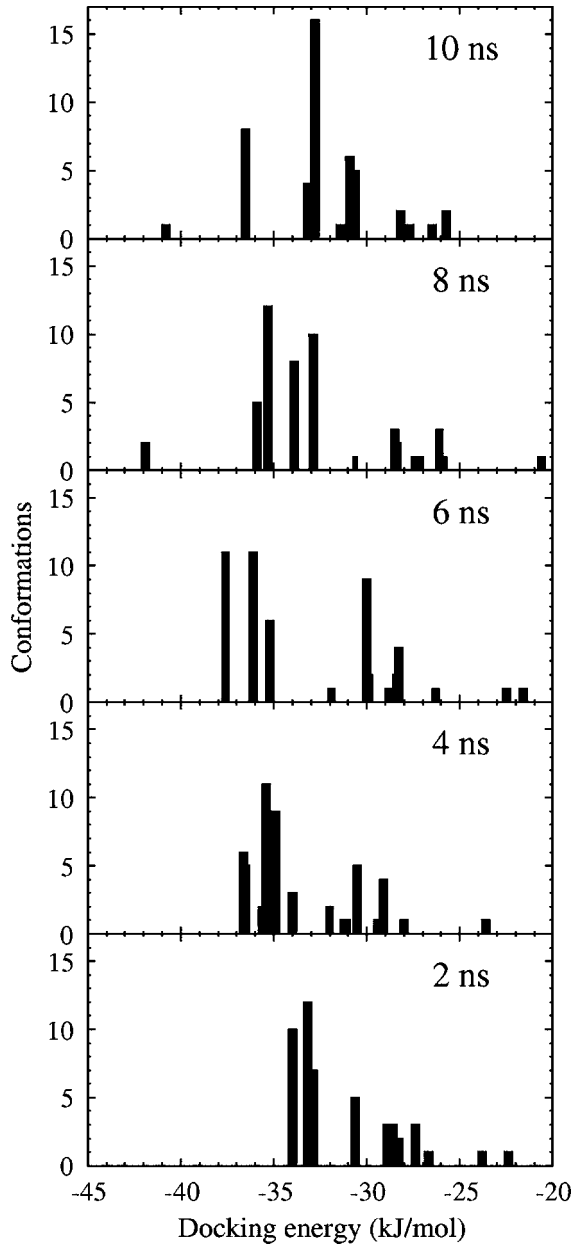

Fig. 3. Populations resulting from the docking of Bip peptide on Bax protein structures obtained at different times along the MD trajectory of Fig. 1. The population was clustered in groups within a RMSD of 1.0 nm and represented as histograms. The docking volume for each time slice was a box of about 150 nm^3 surrounding the whole Bax protein.

we performed a 10 ns MD simulation starting from the above cited configuration with the lowest docking energy. Right side of Figure 5 shows the structure of Bip-Bax binding region after MD. Specifically, stabilizing electrostatic interactions are set between the residue E of Bip with K57 of Bax and between the K residue of

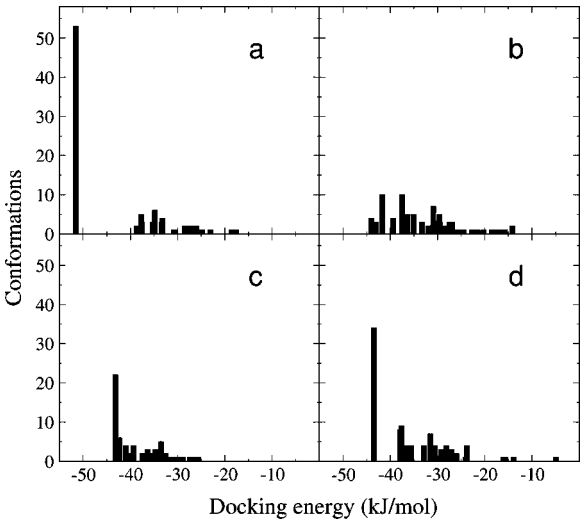

Fig. 4. Populations resulting from the refined docking of Bip peptide to Bax protein. Starting configurations were taken from the four clusters resulting from the docking at 8 ns (Fig. 3), in which Bip had positioned with the lowest energy; the four panels refer to the relative docking regions centered in the peptide and large 30 nm^3 each. Structures are clustered in groups within a RMSD of 0.5 nm.

Bip and E61 of Bax and finally between the amino terminus of Bip with the same residue E61 of Bax. Furthermore a strong hydrogen bond links the oxygen atom of E61 with Hydrogen bound to the Nitrogen atom of the Bip N-terminus. Finally, several favorable hydrophobic contacts also occur.

ED of Bax at 300 and 400 K

Essential dynamics analysis [Amadei et al., 1993] was performed on Bax protein trajectories shown in Figure 1 in the range 1–10 ns at 300 K and 1–5 ns at 400 K, respectively. This method, as described in Methods section, allows a separation of the configurational space into two subspaces: an essential one of very low dimensionality, which is responsible for the main part of the positional fluctuations related to large functional protein motions, and the remaining high dimensional one, characterized by nearly constrained gaussian-like fluctuations related to thermal bath dissipation. The eigenvalues are the averaged squared fluctuations in configurational space along the corresponding directions of the motion (the eigenvectors). The eigenvalues can be sorted in decreasing order and the essential degrees of freedom are identified by the eigenvectors associated to the largest eigenvalues. Table II shows the eigenvalues of all atom coordinates covariance matrices at 300 K and 400 K. The first two eigenvalues for each temperature

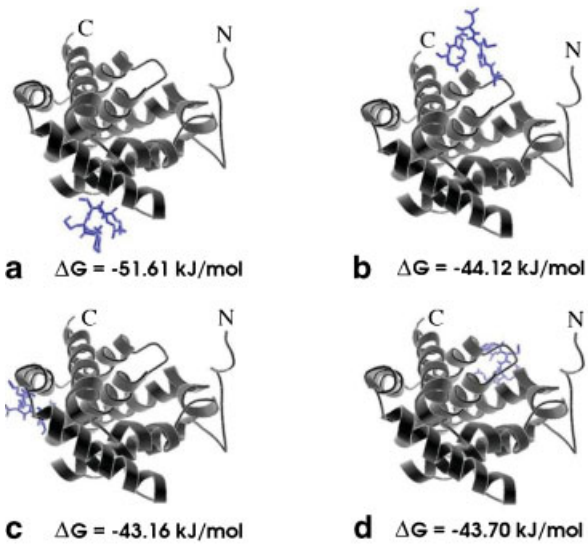

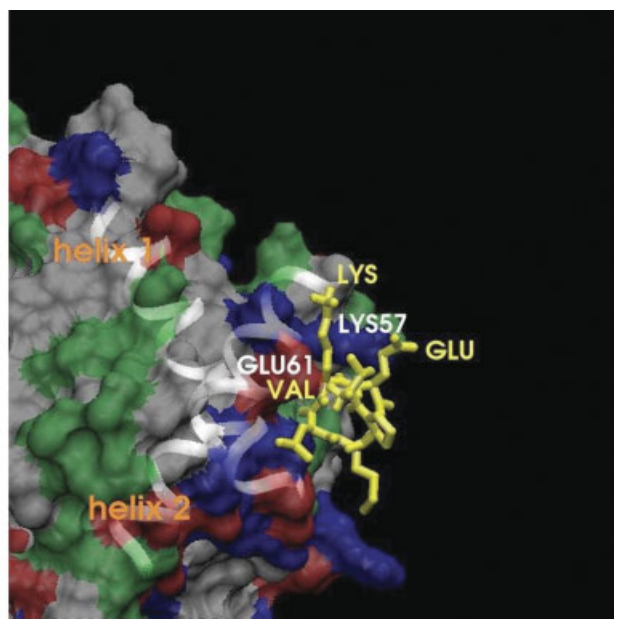

Fig. 5. **Left**: Molecular structures of Bax complexed with Bip peptide as resulting from the automated dockings indicated in Figure 4, with their relative docking free energies. Each configuration corresponds to the lowest energy cluster of Figure 4, for each explored region. **Right**: Details of the interface between Bip and Bax molecules in the complex as resulting after MD simulation starting from the lowest docking energy configuration (region *a* of Fig. 4) and using the simulation parameters indicated in the methods section. [Color figure can be viewed in the online issue, which is available at www.interscience.wiley.com.]

TABLE II. First Five Eigenvalues Resulting From the Essential Molecular Dynamics Analysis of Bax, in the Three Specified Cases of 300 K, 400 K, and in Complex With Bip Peptide

Eigenvalue	300 K	400 K	Bax-Bip
1	20.4275	34.2493	5.38626
2	9.67524	24.6185	2.89322
3	3.7563	8.0839	1.87854
4	3.00246	4.80289	1.25146
5	2.36471	4.45	1.09366

appear to be the most relevant part of the essential motions for both temperatures. The lower part of Figure 6 shows the absolute values of the projection of the indicated eigenvectors of Bax. Specifically, the plots in the left are relative to the two eigenvectors at 300 K (solid line) and at 400 K (dashed line). On the basis of the comparison with the average value of projection of the standard deviation of the displacement for each residue, that are 0.060 nm and 0.043 nm at 300 K for the eigenvalue 1 and eigenvalue 2, respectively, the essential motion at 300 K of eigenvector 1 seems to be mainly localized in the regions involving the segments 1–18, 34–39, 76–84, 150–158, 152–158, 166–172, 189–192 and for the eigenvector 2 the involving similar positions of such short segments in the sequence: that is, 1–12, 35–37, 52–54, 82–85, 143–146, 153–157, 167–169 and 185, 192. The RMSF projections relative to the eigenvectors 1 and 2 at 400 K evidence motions with larger displacements, as expected because of the higher temperature (the standard deviations were 0.102 nm for the eigenvector 1 and 0.153 for the eigenvector 2, respectively). The flexible regions are localized in seven short segments: 2–13, 35–55, 70–90, 100–105, 148–156, 168–178, and 184–192 for the eigenvector 1. For the case of the eigenvector 2 such segments are: 1–13, 34–46, 75–83, 100–103, 152–156, 165–175, and 187–192. However, the pattern shows some relevant differences compared to that relative at 300 K. To better discriminate the protein regions in which the essential motions are preferentially affected by temperature increase, we have plotted, in the low right side of the Figure 6, the ratio of RMSF projections at 400 K and 300 K for both the eigenvectors after normalization obtained dividing for the corresponding average projection value of the standard fluctuation values relative to each residue of the Bax protein. The protein regions whose motions appear to be sensibilized by temperature increase (400 K) involve the segments 60–66, 76–92, 112-119, and 185–192 (localized inside helices 2, 3, 4, 5, and 9) for the eigenvector 1 and the segments 30–43 and 162–178 for the eigenvector 2, respectively (involving helices 3, 4, 8, 9, and relative loops). However, the larger value of the projection displacements on the average for the eigenvector 1 compared to those relative to the eigenvector 2 indicate that the temperature generally affects strongly the collective motion represented by the eigenvector 1 than that relative to the eigenvector 2. The upper part of Figure 6 shows the projections of α-carbons motions along the eigenvectors corresponding to the data shown in the lower parts of the same figure extracted from trajectory sampled after each 300 ps. The more flexible regions are evidenced by largely separated lines.

ED of Bax-Bip

The trajectory of a 10 ns MD simulation of Bip–Bax complex was analysed by ED algorithms [Amadei et al., 1993] starting from the covariance matrix of atomic displacements, similarly as already shown for not complexed Bax macromolecule. Two eigenvectors contribute mostly to collective motions of the atoms of the protein in the complex. Figure 7 shows at bottom left the RMSF projections relative to these eigenvectors (1 and 2, respectively). Eigenvectors 1 and 2 relative to the not complexed Bax are also reported in the same figure for comparison. At bottom right of the same Figure 7 we plotted the ratio of RMSF projections relative to Bax alone and its complexed form for both the eigenvectors after normalization, obtained dividing by the corresponding average projection value of the standard fluctuation relative to all residues in the protein structure. The left and right upper parts of Figure 7 show the projections of α-carbons motions along the eigenvectors 1 and 2, respectively, extracted from trajectory sampled after each 400 ps. The comparison of data relative to Bax in the absence of binding with Bip indicates that regions characterized by large fluctuations become poorly flexible in the complex: specifically, the segments N-terminus and helices 2, 3, 7, 8, and 9. These observations are more evidenced in the projection of essential motions of α-carbons relative to eigenvectors 1 and 2 of the protein alone and complexed with Bip.

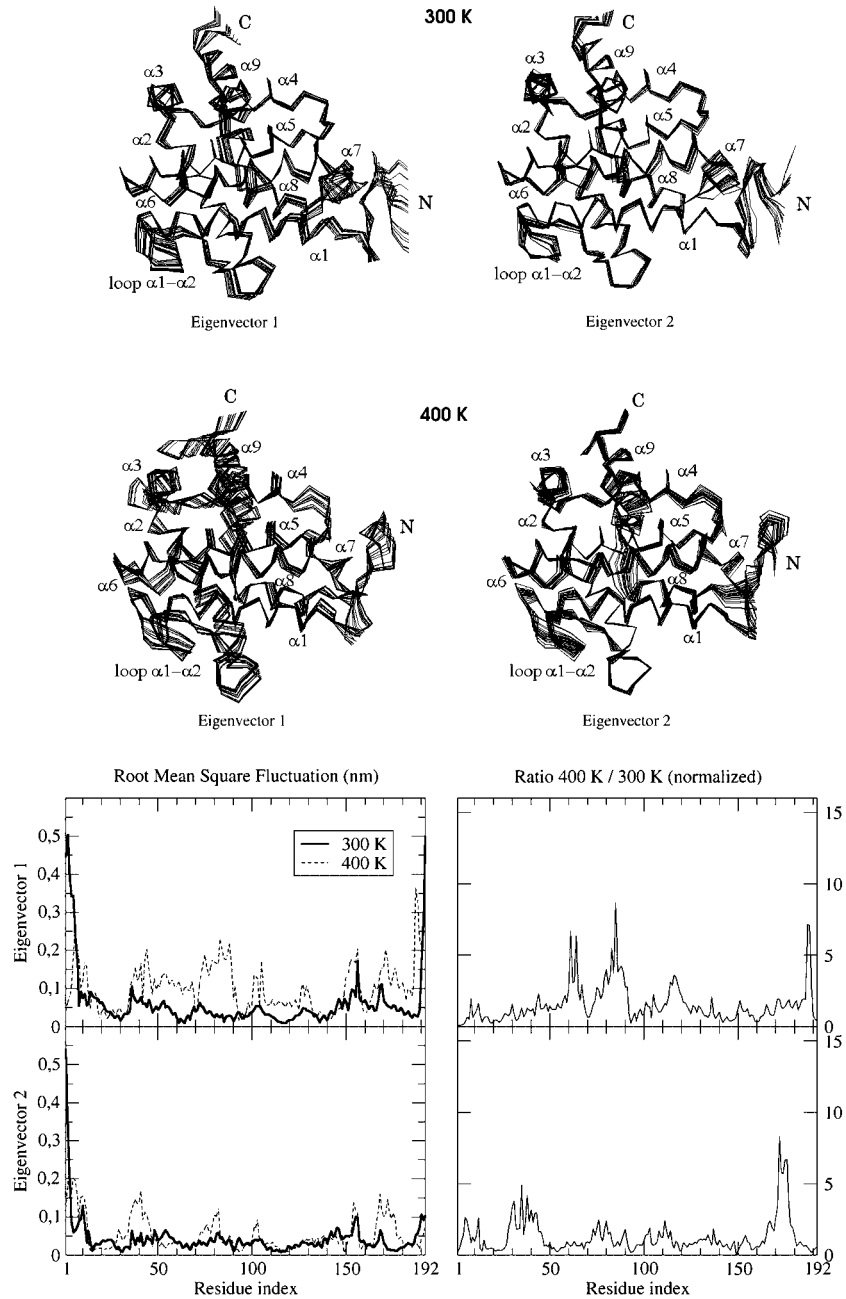

Fig. 6. **Top**: Representation of 20 configurations obtained by projecting the C_α motion onto the eigenvectors 1 and 2, for the two MD calculation temperatures of 300 K and 400 K. Configurations evenly spanned the whole trajectory; secondary structure elements are also indicated. **Bottom left**: Fluctuation along the whole trajectory of the C_α of Bax at 300 K (solid line) and 400 K (dashed line) temperatures, as obtained after projection onto the first two eigenvectors. **Bottom right**: Ratio between the normalized fluctuations of the C_α of Bax protein along the whole trajectory, projected onto the eigenvectors 1 and 2, at the temperatures of 300 K and 400 K. Normalization is obtained, for each temperature and eigenvector, by dividing the fluctuation of each C_α by the average fluctuation of all C_α (see text).

Therefore, the increase in the rigidity in Bip-Bax concerns not only protein segments involved in the binding with Bip but also more distant and functional important regions of Bax.

DISCUSSION

Bax is a crucial regulating protein of Bcl-2 family [Cory and Adams, 1998; Lindeten et al., 2000] that promotes the apoptosis via

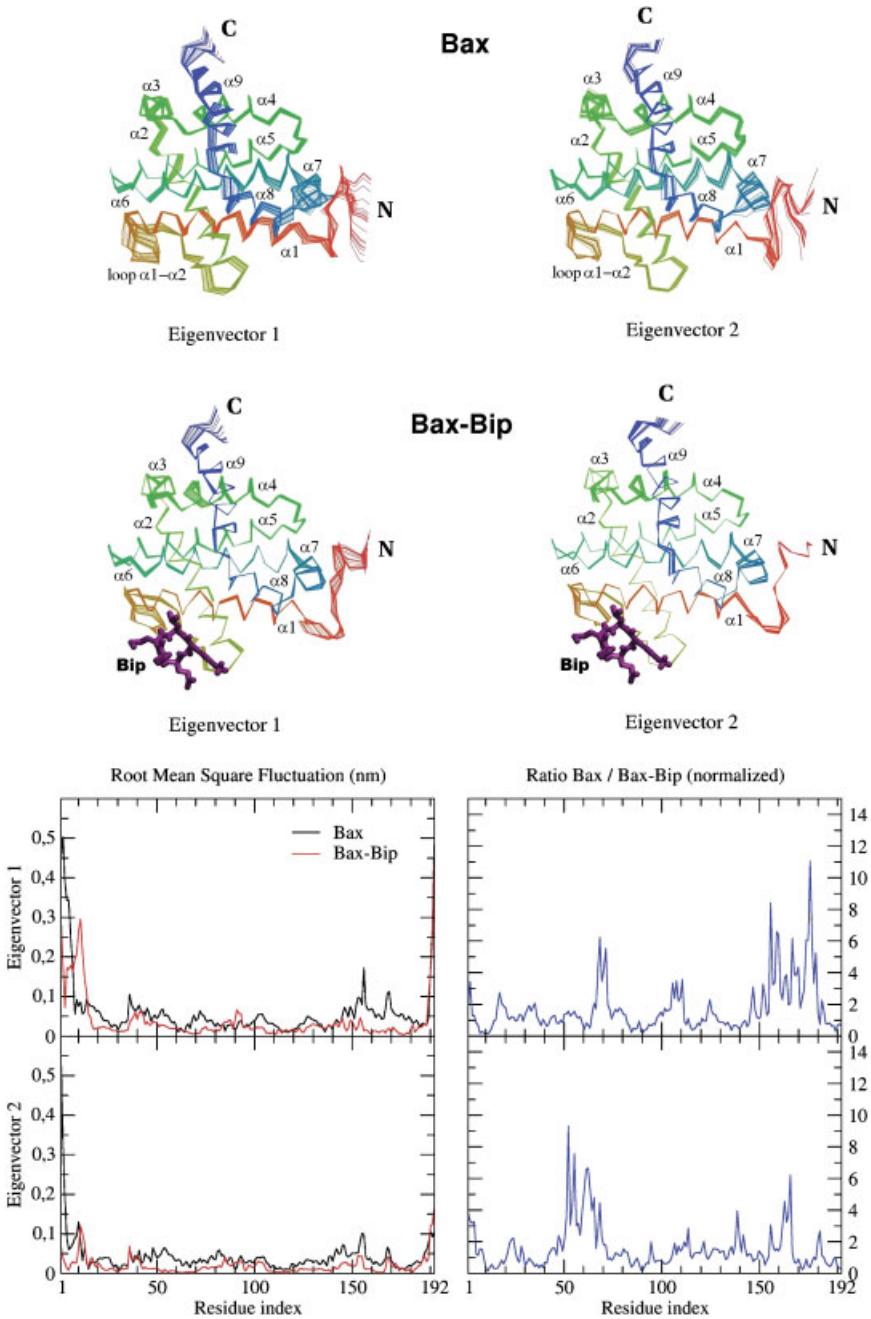

Fig. 7. **Top**: Representation of 20 configurations obtained projecting the C_α motion onto the eigenvectors 1 and 2, for two 10 ns MD simulations relative to Bax alone and complexed to Bip peptide. Configurations evenly spanned the whole trajectory; secondary structure elements are also indicated for each group of configurations. **Bottom left**: Fluctuation along the whole trajectory of the C_α of Bax alone (black) and complexed with Bip peptide (red), as obtained after projection onto the eigenvectors 1 and 2. **Bottom right**: Ratio between the normalized fluctuations of the C_α of Bax protein alone and complexed with Bip peptide, along the whole trajectory, projected onto the eigenvectors 1 and 2. Normalization is obtained, in each case, by dividing the fluctuation of each C_α by the average fluctuation of all C_α (see text). [Color figure can be viewed in the online issue, which is available at www.interscience.wiley.com.]

cytochrome *c* by traslocating from cytosol to mitochondium outer membrane after appropriate stimuli. The ratio between anti-apoptotic proteins such as Bcl-2 relative to pro-cell death proteins such as Bax determines the ultimate sensitivity of cells to various apoptotic stimuli [Hsu et al., 1997; Green and Reed, 1998]. Several pro and anti-apoptotic proteins can

form physical interactions with each other in a complicate network of homo- and heterodimers [Cory and Adams, 1998; Yu and Zhang, 2003]. Several aspects are not well known about structure-function in the Bax protein as pertains mainly to two questions: (a) identification of structural regions of the protein involved in homodimerization and heterodimerization with anti-apoptotic proteins; (b) to identify the protein regions and the motions of Bax induced by apoptotic stimuli that are involved in the conformational change that targets Bax into the mitochondria external membrane. The combined action of molecular dynamic simulation and automated docking, as shown in the Results, can give information about both the above reported questions. The regulation of Bax function via heterodimer formation has been investigated for the specific case of a Bax-inhibiting exa-peptide. This peptide belonging to the segment 578–587 of the anti-apoptotic protein Ku70 [Walker et al., 2001; Sawada et al., 2003b] (and other short peptides corresponding to the same Ku70 regions but differing in few residues) has been demonstrated to be sufficient for the inhibition of Bax action. Actually it is not clear if Bip can bind Bax directly. To support this idea and also find the best region of Bax protein showing highest affinity for Bip peptide the docking procedure was performed in multiple steps. With an appropriate partitioning of the volume surrounding Bax macromolecule we explored the whole surface of Bax by automatic docking. However, AutoDock 3.0 searching considers a fixed structure for the macromolecule. To take into account for the Bax internal flexibility, we performed a preliminary rough docking of Bip with Bax structures resulting from MD trajectory at 300 K at each 1 ns interval (with the exclusion of the first one). On going from simulation time of 2–10 ns the clustered structures of Bip-Bax complex decreased their binding energy and at 8 ns a single binding site showed the highest affinity. The affinity of this binding site, located in proximity of the N-terminus and α1-helix furtherly increased after more refined dockings in which the search was performed on a limited area of Bax surface surrounding the preliminarly determined binding site and allowing a larger flexibility for Bip. The obtained free energy of binding is high (corresponding to docking energy of -51.56 kJ/mol) and strongly supports the idea that the Bip inhibition of apoptotic Bax action occurs by direct binding of Bip to Bax molecule. This binding, involving the N terminus of Bax, inhibits the conformational change of this protein region, hypothesized to occur in activated Bax, after that the protein translocates to the mitochondria. This conclusion explains the experimental reports that the deletion of N terminus results in direct targeting of Bax to the mitochondria [Oltvai and Korsmeyer, 1994]. Other reports suggest that a conformational change in the N terminus, resulting in cytochrome c release and amplification of apoptotic cascade, is caused by Bid, a pro-apoptotic molecule [Goping et al., 1998], or by a detergent (residues 14–24 in N terminus of Bax) [Gross et al., 1998]. Finally, it has been reported recently that also the activation of the Fas receptor induces a conformational change in the N terminus of Bax, which appears to precede its translocation to the mitochondria [Murphy et al., 2000].

MD simulation at 400 K was performed to search among thermal amplified protein motions those involving regions of Bax with potential functional effects, that is, that can induce Bax activation after apoptotic stimuli. Protein motions consist of thermal fluctuations and collective motions related to function. Thus the "random" motions are indeed filtered out. This can be done by ED analysis, leaving the most important correlated motions. The protein region in which the flexibility was particularly amplified by the 100 K increase in temperature is evidenced in Figure 6. The essential behavior is mainly located in at the BH3 binding site but high mobility is also visible for the N- and C-terminal. Moreover, the most hydrophobic helix 6 and the helix 5 appear strongly perturbed by temperature increase. Other particularly affected regions are the helix 7 that unfolds and the helix 9 that shortens and also seems to move out of the hydrophobic groove. This movement is particularly important because the opening of the hydrophobic groove by displacement of the α9 helix is necessary to allow the interaction of the prominent BH3 domain of anti-apoptotic molecules such Bcl-x_L or Bcl2 in heterodimer complex or of the BH3 of the same Bax molecule after activation by apoptotic stimuli in the auto-oligomerization process supposed to occur for the pore formation at the mitochondria membrane [Scorrano et al., 2004; Terrones et al., 2004].

Finally the comparison of the collective motions, as evidenced by essential analysis, occurring in Bax complexed or not with Bip exapeptide (Fig. 7) evidences that the binding with Bip strongly reduces the mobility of BH3 domain directly involved in the binding, but also shifts and makes rigid or less mobile distant protein regions such as helix 9 that allows, as already described, the access to the hydrophobic bundle formed by helices 4-8. Finally, N and C termini, considered very important in determining the interaction with the external membrane of mitochondria, also become less oscillating. Further functional and molecular dynamic comparative studies of Bax interaction with short peptides in which appropriate changes in the sequence will be introduced that could be relevant to therapeutic anti-cancer applications by regulating Bax function in apoptosis.

ACKNOWLEDGMENTS

This work was supported by the Italian Ministry of University and Scientific and Technology Research (PRIN2004 "Study of the expression, activity and intracellular compartmentalization of signaling proteins in tumor cells exposed or not to biological and cytotoxic agents: a genomic and proteomic approach").

REFERENCES

Amadei A, Linsenn ABM, Berendsen HJC. 1993. Essential dynamics of proteins. Proteins 17:412–425.

Berendsen HJC, Postma JPM, van Gunsteren WF, Di Nola A, Haak R. 1984. Molecular dynamics with coupling to external bath. J Chem Phys 81:3684–3690.

Cory S, Adams JM. 1998. The Bcl-2 protein family: Arbiters of cell survival. Science 281:1322–1326.

Danial NN, Korsmeyer SJ. 2004. Cell death: Critical control points. Cell 116:205–219.

Earnshow WC, Martins LM, Kaufmann HF. 1999. Mammalian caspases: Structure, activation, substrates and functions during apoptosis. Ann Rev Biochem 68:383–424.

Gasteiger J, Marsili M. 1980. Iterative partial equalization of orbital electronegativity: A rapid access to atomic charges. Tetrahedron 36:3219–3228.

Goping IS, Gross A, Lavonie JN, Nguyen M, Jemmerson R, Roth K, Korsmeyer SJ, Shore GC. 1998. Regulated targeting of Bax to mitochondria. J Cell Biol 143:207–215.

Green DR, Reed C. 1998. Mitochondria and apoptosis. Science 281:1309–1312.

Gross A, Jockel J, Wie MC, Korsmeyer SJ. 1998. Enforced dimerization of Bax results in its translocation, mitochondrial dysfunction and apoptosis. EMBO J 17:3878–3885.

Hess B, Bekker H, Berendsen HJC, Fraaije JGEM. 1997. LINCS: A linear constraint solver for molecular simulations. J Comp Chem 18:1463–1472.

Hsu YT, Walker G, Youle RJ. 1997. Cytosol-to-membrane redistribution of Bax and Bcl-x_L. Proc Natl Acad Sci USA 94:3668–3672.

Jiang X, Wang X. 2004. Cytochrome c-mediated apoptosis. Annu Rev Biochem 73:87–106.

Koradi R, Billiter M, Wütrich K. 1996. MOLMOL: A program for display and analysis of macromolecular structures. J Mol Graph 14:51–55.

Lindahl E, Hess B, van der Spoel D. 2001. GROMACS 3.0: A package for molecular simulation and trajectory analysis. J Mol Model 7:306–317.

Lindeten T, Ross AJ, King A, Zong WX, Rathmell JC, Shiels HA, Ulrich E, Waymare KG, Mahar P, Frauwirth K, Chen Y, Wei M, Eng VM, Adelman DM, Simon MC, Ma A, Golden JA, MacGregor GR, Thompson CB. 2000. The combined function of proapoptotic Bcl-2 family members Bak and Bax are essential for normal development of multiple tissues. Mol Cell 6:1389–1399.

Luty BA, Tironi IG, van Gunsteren WF. 1995. Lattice-sum methods for calculating electrostatic interactions in molecular simulations. J Chem Phys 103:3014–3021.

Matson MP. 2000. Apoptosis in neurodegenerative disorders. Nat Mol Cell Biol 1:120–129.

Mikhailov V. 2003. Association of Bax and Bak homooligomers in mitochondria. J Biol Chem 278:5367–5376.

Morris GM, Goodsell DS, Halliday RS, Huey R, Hart WE, Belew RK, Olson AJ. 1998. Automated docking using a Lamarkian genetic algorithm and an empirical binding free energy function. J Comp Chem 14:1639–1662.

Murphy KM, Streips UN, Lock RB. 2000. Bcl-2 inhibits a Fas induced conformational change in Bax terminus and Bax mitochondrial translocation. J Biol Chem 275:17225–17228.

Nam Y, Mani K, Ashton AW, Peng CF, Krishnamurthy B, Hayakawa Y, Lee P, Korsmeyer SJ, Kitsi RN. 2004. Inhibition of both the extrinsic and intrinsic death pathways through nonhomotypic death-fold interactions. Mol Cell 15:901–912.

Oltvai Z, Korsmeyer SJ. 1994. Checkpoints of dueling dimers foil death wishes. Cell 79:189–192.

Petros AM, Olejniczak ET, Fesik SW. 2004. Structural biology of Bcl-2 family of proteins. Biochim Biophys Acta 1644:83–94.

Saito M, Korsmeyer SJ, Schlesinger PH. 2000. Bax-dependent transport of cytochrome *c* reconstituted in pure liposomes. Nat Cell Biol 2:553–555.

Sanner MF, Duncan BS, Carrillo CJ, Olson AJ. 1999. Integrating computation and visualization for biomolecular analysis: An example using Python and AVS. Proc Pac Symp Biocomput 4:401–412.

Sawada M, Sun W, Hayes P, Leskov K, Boothman DA, Matsuyama S. 2003a. Ku70 suppresses the apoptotic translocation of Bax to mitochondria. Nat Cell Biol 5:320–329.

Sawada M, Hayes P, Matsuyama S. 2003b. Cytoprotective membrane-permeable peptides designed from the Bax-binding domain of Ku70. Nat Cell Biol 5:352–357.

Schmitt CA. 2003. Senescence, apoptosis and therapy: Cutting the lifelines of cancer. Nat Cancer 3:286–295.

Scorrano L, Oakes SA, Opferman EHC, Cheng EH, Sarcinell MD, Pozzan T, Korsmeyer SJ. 2004.

Membrane-insertion fragments of Bcl-x_L, Bax, and Bid. Biochemistry 43:10930–10943.

Suzuki M, Youle MS, Tjandra N. 2000. Structure of Bax: Coregulation of dimer formation and intracellular localization. Cell 105:645–654.

Terrones O, Antonsson B, Yamaguchi H, Wang HG, Liu J, Lee RM, Herrmann A, Basañez G. 2004. Lipidic pore formation by the concerted action of pro-apoptotic Bax and tBid. J Biol Chem 279:30081–30091.

Van der Spoel D, Lindhal E, Hess B, van Buuren AR, Apol E, Muelenhoff PJ, Tieleman DP, Sijbers ALTM, Fenstra KA, van Drunen R, Berendsen HJC. 2004. Gromacs User Manual Version 3.2 www.gromacs.org

Walker JR, Corpina RA, Goldberg J. 2001. Structure of the Ku heterodimer bound to DNA and its implicxations for double-strand break repair. Nature 412:607–614.

Yu J, Zhang L. 2003. Apoptosis in human cancer cells. Curr Opin Oncol 16:19–24.

Zha H, Almè-Sempè C, Sato T, Reeds J. 1996. Pro-apoptotic protein Bax heterodimerizes with Bcl-2 and homodimerizes with Bax via a novel domain (BH3) distinct from BH1 and BH2. J Biol Chem 271:7440–7444.